31st Annual International Conference of the IEEE EMBS
Minneapolis, Minnesota, USA, September 2-6, 2009

Quantification of SPIO Nanoparticles using Phase Gradient Mapping

Jason Langley, *Student Member, IEEE* and Qun Zhao*, *Senior Member, IEEE*

***Abstract*—A new method is developed to quantify the concentration of super-paramagnetic iron oxide (SPIO) contrast agent using magnetic resonance imaging (MRI). The proposed method utilizes a positive contrast method, known as phase gradient mapping (PGM), to find the gradient of the field map. Then the concentration is calculated by fitting the gradient of the field map to the gradient of an ideal geometric model. The proposed method was compared to relaxivity-based SPIO quantification method and was applied to calculate the concentration of SPIO contrast agent for MRI experiments performed on a phantom with known concentrations. The results obtained from the proposed method accord well with the true concentrations.**

I. Introduction

SUPER-paramagnetic iron oxide (SPIO) nanoparticles generate a strong susceptibility gradient that makes them an ideal contrast agent in magnetic resonance imaging (MRI). Contrast agents based on SPIO nanoparticles are ideally suited for a wide range of applications ranging from *in vivo* cell tracking to tumor enhancement. The quantification contrast agents based on SPIO nanoparticles becomes a pressing issue as contrast agents based on SPIO nanoparticles become more prevalent in MRI.

Contrast agents based on SPIO nanoparticles change the relaxivity of the tissue and cause signal decay in T_2^*-weighted MR images. The signal decay causes a signal void (a "dark spot") in the region containing SPIO nanoparticles; this is known as negative contrast. Signal loss associated with negative contrast images makes *in vivo* identification of SPIO nanoparticles difficult as signal loss is also associated with air pockets or tissue interfaces containing significant susceptibility differences. Positive contrast techniques attempt to remove the ambiguity caused by the signal loss by generating high-intensity signals (a "bright spot"). Many existing positive contrast techniques are able to detect the presence of SPIO nanoparticle-based contrast agents. However, very few of the existing positive contrast techniques can quantify the amount of SPIO nanoparticles within a given structure.

Positive contrast methods can be broken into two categories. The first category of positive contrast methods uses modified pulse sequences to produce positive contrast. Examples of these techniques include the white marker method [1], inversion recovery on resonance water suppression (IRON) [2], an off-resonance technique [3], and gradient echo acquisition for super-paramagnetic particles (GRASP) [4]. These techniques require *a priori* knowledge of the distribution of the magnetic field inhomogeneities.

The second category of positive contrast methods use post-processing algorithms to generate positive contrast in regular MR images. Examples of positive contrast or SPIO detection algorithms in this category include phase gradient mapping (PGM) [5], susceptibility gradient mapping (SGM) [6, 7], and phase map cross-correlation detection and quantification (PDQ) [8]. As the name suggests, SGM generates positive contrast from susceptibility gradients that are induced by changes in tissue. PDQ detects SPIO nanoparticles by modeling the magnetic field inhomogeneities generated by the nanoparticles as point dipoles. PDQ uses a cross-correlation method to match the magnetic field of a point dipole to the magnetic field generated by the SPIO nanoparticles. While PDQ is able to pinpoint the approximate location of the nanoparticles, no quantification is performed on the image.

Most SPIO quantification methods [9-11] rely on mapping the relaxation rate in a particular region. The relaxation rate is defined to be $1/T_2^*$ and is denoted R_2^*. These methods assume that R_2^* varies linearly with SPIO concentration. The equation that governs how the relaxation rate changes with concentration is

$$R_2^* = R_{20}^* + r_2^* c \tag{1}$$

where R^*_{20} denotes the intrinsic relaxation rate (e.g. no contrast agent), r_2^* denotes the relaxivity of the contrast agent, and c denotes the concentration of the contrast agent. The relaxation rate method is susceptible to B_0 inhomogeneities, eddy currents, and gradient instabilities [12].

Another SPIO quantification method is Dixon's quantification method [13]. Dixon's quantification method models the magnetic field inhomogeneities created by the SPIO nanoparticles as point dipoles. The concentration of nanoparticles is quantified by fitting the model to the data. One drawback of Dixon's quantification method is that it relies on phase unwrapping to generate the field map.

In this work, we propose a SPIO nanoparticles quantification method that requires no phase unwrapping step. We apply the positive contrast technique PGM to the

Manuscript received April 6, 2009.

Jason A. Langley is with the Department of Physics and Astronomy and the BioImaging Research Center (BIRC), the University of Georgia, Athens, GA 30602 USA (e-mail: impulse@ physast.uga.edu).

Qun Zhao is with the Department of Physics and Astronomy and the BioImaging Research Center (BIRC), the University of Georgia, Athens, GA 30602 USA (phone: 706-583-5558; fax: 706-542-2492; e-mail: qzhao@physast.uga.edu)

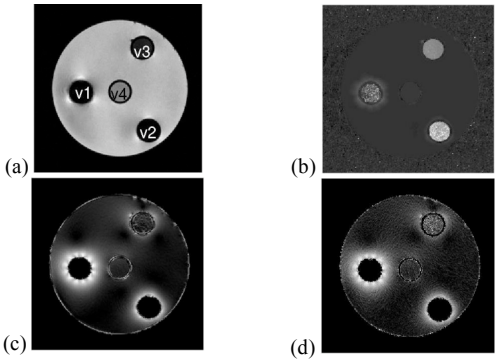

Fig. 1. (a) Magnitude image of the agar phantom. Each vial contains different concentrations of Ferumoxides. (b) A map of the R_2^* values for the agar phantom. (c) The corresponding phase gradient map of the agar phantom. in the high SNR regime. (d) The phase gradient map of the agar phantom in the low SNR regime.

problem of quantification of SPIO nanoparticles. The magnetic field inhomogeneity is modeled as the field from a simple geometry (e.g. cylinder, sphere) and the PGM map is compared with the gradient of the magnetic field induced by susceptibility differences between the simple geometry and the surrounding area. MR experimental results were obtained from a phantom with imbedded vials of known SPIO concentrations.

II. Phase Gradient Mapping

Magnetic field inhomogeneities are generated by susceptibility differences between a region containing SPIO nanoparticles and the areas surrounding the region containing the nanoparticles. The magnetic field inhomogeneities dephase spins in voxels neighboring the nanoparticles. The dephasing caused by the SPIO nanoparticles creates a signal void in the magnitude image and creates phase disturbances in the phase map. The PGM method creates a positive contrast by mapping the rapidly changing phase in regions neighboring SPIO nanoparticles. In the phase gradient map, areas with higher concentrations of SPIO nanoparticles should have a larger phase gradient than areas with lower concentrations of SPIO nanoparticles. Ideally, areas without nanoparticles should have no phase gradient.

There are a number of ways to calculate the phase gradient [5, 14, 15]. In this work, we apply a phase gradient calculation method that calculates the phase gradient in k-space [14]. The phase gradient is calculated directly from the complex valued image, denoted $\rho(x,y)$. The complex valued image can be broken into phase maps, denoted $\varphi(x,y)$, and magnitude images. The x-component of the phase gradient is calculated using the equation

$$\frac{\partial\varphi(x,y)}{\partial x} = -i\bar{\rho}^{c}(x,y)\frac{\partial\bar{\rho}(x,y)}{\partial x} \tag{2}$$

where x^c denotes the complex conjugate of x, $\bar{\rho}(x,y) = \rho(x,y)/|\rho(x,y)|$, and the expression for the partial derivative normalized image is

TABLE I
SNR for the Center Slice of Each Acquisition

	TE_1	TE_2	TE_3	TE_4	TE_5
SNR without Gaussian Noise	70	73	72	75	73
SNR with Gaussian Noise	9	10	10	10	10

The top row displays the SNR for the center slice of each acquisition before Gaussian noise was added to each phase map. The bottom row displays the SNR for the center slice after Gaussian noise was added to each phase map.

$$\frac{\partial\bar{\rho}(m,n)}{\partial x} = \sum_{p=-N_x/2}^{N_x/2-1}\frac{i2\pi p}{N_x^2}\mathrm{DFT}(\bar{\rho}(p,n))e^{i2\pi mp/N_x} \tag{3}$$

where the discrete Fourier Transform (DFT) of the $\bar{\rho}(x,y)$ is

$$\mathrm{DFT}(\bar{\rho}(p,n)) = \sum_{m=-N_x/2}^{N_x/2-1}\bar{\rho}(m,n)e^{-i2\pi mp/N_x}. \tag{4}$$

The y-component of the phase gradient has a similar structure. A Hamming window was applied as a spatial smoothing step to the entire column during the calculation of the phase gradient to remove Gibbs ringing effect.

III. SPIO Quantification using PGM

The field map of a given image displays the z-component (parallel to B_0, the main magnetic field) of magnetic field inhomogeneities. The field map of an image is constructed from two phase maps taken at different echo times (TE). The field map of an image can be represented mathematically as

$$\Delta B(x,y) = \frac{\varphi_1(x,y) - \varphi_2(x,y)}{\gamma\Delta TE} \tag{5}$$

where γ denotes the gyromagnetic ratio for hydrogen and ΔTE denotes the difference between two echo times. The x-component of the gradient of $\Delta B(x,y)$ is

$$\frac{\partial\left(\Delta B(x,y)\right)}{\partial x} = \frac{1}{\gamma\Delta TE}\left(\frac{\partial\varphi_1(x,y)}{\partial x} - \frac{\partial\varphi_2(x,y)}{\partial x}\right). \tag{6}$$

A similar relationship holds for the y-component of the gradient of $\Delta B(x,y)$. The phase gradients can be calculated using the PGM method described in the previous section.

The strength of the induced magnetic field in an infinitively long cylinder depends on the magnetic moment of the cylinder and the angle the cylinder makes with B_0. In regions outside of the cylinder, the magnetic field inhomogeneity induced by the cylinder has a spatial dependence of

$$\Delta B(x,y) = \left(\frac{\mu_0 m}{2}\right)R^2\sin^2\theta\frac{x^2-y^2}{\left(x^2+y^2\right)^2} \tag{7}$$

where θ denotes the angle the cylinder makes with B_0, R denotes the radius of the cylinder, and m denotes the magnetic moment per unit volume of the induced magnetic field. The partial derivatives of the induced magnetic field are

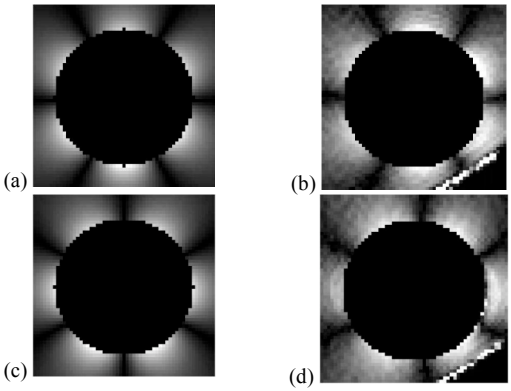

Fig. 2. (a) A plot of the absolute value of the surface described by (6). (b) A plot of the absolute value of the *x*-component of the phase gradient map for vial v2 in the high SNR regime. (c) A plot of the absolute value of the surface described by (7). (d) A plot of the absolute value of the *y*-component of the phase gradient map for vial v2 in the high SNR regime.

$$\frac{\partial\left(\Delta B(x,y)\right)}{\partial x} = -xm\mu_0 R^2 \sin^2\theta \frac{x^2 - 3y^2}{\left(x^2 + y^2\right)^3} \tag{8}$$

and

$$\frac{\partial\left(\Delta B(x,y)\right)}{\partial y} = ym\mu_0 R^2 \sin^2\theta \frac{y^2 - 3x^2}{\left(x^2 + y^2\right)^3}. \tag{9}$$

The center of the infinite cylinder is obtained by fitting the measured induced magnetic field gradients using the PGM method and the theoretical gradient of the induced magnetic field. The concentration of the SPIO based contrast agent is determined by using PGM to construct the gradient of the field map and comparing the gradient of the field map with the gradient of the model. To minimize the error associated with the calculation of the contrast agent, the calculation should only be performed in regions with a significant phase gradient.

IV. Methods

A. Data Acquisition

An agar phantom was constructed with four vials embedded within the phantom. Each vial contained a different concentration of Ferumoxides (Berlex Laboratories, Wayne, NJ), a contrast agent based on SPIO nanoparticles. Each vial within the phantom was offset with a different angle relative to B_0. The concentration of Ferumoxides in each vial and the angle each vial made with B_0 is shown in Table I. The contrast agent generates 68 emu / g Fe and has a relaxivity of 160 s^{-1} at 0.47 T [15].

The phantom data set was acquired using a whole-body Philips 3T Achieva clinical MR scanner (Phillips Medical Systems, Best, the Netherlands). Multiple 2D gradient echo images were acquired at five different echo times: TE_1= 5 ms, TE_2 = 15 ms, TE_3 = 25 ms, TE_4 = 35 ms, TE_5 = 45 ms. Each acquisition had the following parameters: TR = 50 ms, flip angle = 25 degrees, slice thickness = 1 mm, FOV = 70 mm, 256×256 acquisition matrix, 24 axial slices.

TABLE II
Properties of the Agar Phantom In the High SNR Regime

Vial	Concentration (ug/ml)	Angle	Proposed Method (ug/ml)	Relaxivity Method (ug/ml)
v1	160	11.6°	136.73 ± 8.01	-
v2	80	5.3°	80.18 ± 11.74	77.16 ± 18.56
v3	40	3.6°	36.85 ± 7.62	45.67 ± 3.34

The calculated properties for the agar phantom data set in the high SNR regime.

B. Data Processing

To calculate the concentration of the contrast agent within the vials, we modeled the cylindrical vials as infinite cylinders. Slices were chosen near the center (in the longitudinal direction) of each vial to preserve the infinite cylinder approximation. To evaluate the performance of the SPIO quantification algorithm in an environment with low SNR, Gaussian noise was added to the real and imaginary parts of the k-space data set. The noisy image was transformed into image space by a 2D fast Fourier transform was applied to the modified k-space data.

The SNR for the center slice of each acquisition is displayed in Table I. The SNR was calculated as $S_0/(1.53\sigma_N)$, where S_0 is the mean of a homogeneous area away from the vials within the phantom and σ_N is the mean of the standard deviation of four areas outside the phantom. The SNR for the center slice of each acquisition after the addition of Gaussian noise is also displayed in Table I

For the high SNR regime and the low SNR regime, the gradient of the field map was constructed using the phase maps acquired at echo times TE_1 and TE_2. The relaxivity-based SPIO quantification method based on eq. (1) used all five phase maps to calculate the concentration. The relaxivity of the phantom was found by performing a least squares fit on the relaxation rates from the vials.

The PGM algorithm, the proposed SPIO quantification method, and relaxivity-based SPIO quantification method were implemented in MATLAB (The MathWorks, Natick, Massachusetts) and executed on a Red Hat Enterprise Linux server equipped with a 2.6-GHz dual core Intel Xenon CPU.

V. Results and Discussion

The results of the proposed SPIO quantification algorithm applied to the phantom data sets in the high SNR regime are shown in Table II. The results of the proposed quantification algorithm accord well with the results from the relaxivity-based quantification method and the known concentrations in each vial. The results of the SPIO quantification algorithm in the low SNR regime are shown in Table III. As expected, the standard deviation of the calculated concentration increased as more noise was introduced to the original gradient echo images.

We were unable to calculate the value of R_2^* for the vial with the highest concentration since the signal received from the vial was at the noise level for all five acquisitions due to strong magnetic susceptibility effect. The application of algorithms developed for ultrashort TEs can mitigate this problem [16].

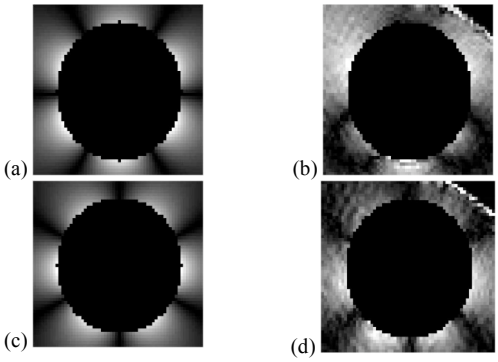

Fig. 3. (a) A plot of the absolute value of the surface described by (6). (b) A plot of the absolute value of the *x*-component of the phase gradient for the vial with concentration 40 ug/ml in the high SNR regime. (c) A plot of the absolute value of the surface described by (7). (d) A plot of the absolute value of the *y*-component of the phase gradient for the vial with concentration 40 ug/ml in the high SNR regime.

The induced magnetic field gradients generated by the vials accord well with the theoretical predictions of the infinite cylinder model at moderate to high concentrations of the contrast agent. However, at low concentrations the contrast agent does not generate a measurable field to produce a useful phase gradient in the *x*-direction. At low concentrations, the contrast agent generated a phase gradient in the *y*-direction adequate enough to perform the quantification procedure. The deficiency in the measurable field in the low concentration vial is shown in Fig. 3.

For this experiment, the infinite cylinder model gives a good approximation of the experimental geometry. Other models that have closed-form magnetic fields can be substituted in place of the infinite cylinder model. For example, the use of a spherical model would be appropriate if the SPIO nanoparticles were embedded within a spherical structure. Eventually we hope to implement the SPIO quantification algorithm using numerical techniques in place of the closed-form models that are currently in the quantification algorithm. The numerical techniques will allow us to calculate the magnetic field induced by arbitrary geometries and apply the quantification algorithm to different physiological applications.

VI. Conclusion

A new SPIO quantification algorithm is introduced. The proposed quantification algorithm performs well in high SNR conditions. At extremely low SNR, the proposed quantification algorithm gives an adequate measure of the concentration of contrast agent in the phantom. The results of the proposed quantification algorithm agree with the known concentration in the phantom test.

Acknowledgment

The Authors would like to thank Dr. Wei Liu for providing the phantom data set.

References

[1] J.H. Seppenwoolde, K.L. Vincken, and C.J. Bakker, "White-marker imaging--separating magnetic susceptibility effects from partial volume effects," *Magnetic Resonance in Medicine*, vol. 58, (no. 3), pp. 605-609, 2007.

[2] M. Stuber, W. GIlson, M. Schär, D. Kedziorek, L. Hofmann, S. Shah, E.J. Vonken, J.W.M. Bulte, and D.L. Kraitchman, "Positive conreast visualization of iron oxide-labeled stem cells using inversion-recovery with ON-resonant water suppression (IRON)," *Magnetic Resonance in Medicine*, vol. 58, (no. 5), pp. 1072-1077, 2007.

[3] C.H. Cunningham, T. Ari, P.C. Yang, M.V. McConnell, J.M. Pauly, and S.M. Conolly, "Positive contrast magnetic resonance imaging of cells labeled with magnetic nanoparticles," *Magnetic Resonance in Medicine*, vol. 53, (no. 5), pp. 999-1005, 2005.

[4] V. Mani, K.C. Briley-Saebo, V.V. Itskovich, D.D. Samber, and Z.A. Fayad, "Gradient echo acquisition for superparamagnetic particles with positive contrast (GRASP): Sequence characterization in membrane and glass superparamagnetic iron oxide phantoms at 1.5T and 3T," *Magnetic Resonance in Medicine*, vol. 55, (no. 1), pp. 126-135, 2005.

[5] C.J. Bakker, H. de Leeuw, K.L. Vincken, E.J. Vonken, and J. Hendrikse, "Phase gradient mapping as an aid in the analysis of object-induced and system-related phase perturbations in MRI," *Phys Med Biol*, vol. 53, (no. 18), pp. N349-58, Sep 21 2008.

[6] H. Dahnke, W. Liu, D. Herzka, J.A. Frank, and T. Schaeffter, "Susceptibility gradient mapping (SGM): A new postprocessing method for positive contrast generation applied to superparamagnetic iron oxide particle (SPIO)-labeled cells," *Magnetic Resonance in Medicine*, vol. 60, (no. 3), pp. 595-603, 2008.

[7] Wei Liu, H. Dahnke, E.K. Jordan, T. Schaeffter, and J.A. Frank, "In vivo MRI using positive-contrast techniques in detection of cells labeled with superparamagnetic iron oxide nanoparticles," *NMR in Biomedicine*, vol. 21, (no. 3), pp. 242-250, 2008.

[8] P.H. Mills, Y.-J.L. Wu, C. Ho, and E.T. Ahrens, "Sensitive and automated detection of iron-oxide-labeled cells using phase image cross-correlation analysis," *Magnetic Resonance Imaging*, vol. 26, pp. 618-628, 2008.

[9] R. Kuhlpeter, H. Dahnke, L. Matuszewski, T. Persigehl, A.c. Wallbrunn, T. Allkemper, W.L. eindel, T. Schaeffter, and C. Bremer, "R2 and R2* mapping for sensing cell-bound superparamagnetic nanoparticles," *Radiology*, vol. 245, (no. 2), pp. 449-457, 2007.

[10] A.M. Rad, A.S. Arbab, A.S.M. Iskander, Q. Jiang, and H. Soltanian-Zadeh, "Quantification of superparamagnetic iron oxide (SPIO)-labeled cells using MRI," *Journal of Magnetic Resonance Imaging*, vol. 26, pp. 366-374, 2007.

[11] C.V. Bowen, X. Zhang, G. Saab, P.J. gareau, and B.K. Rutt, "Application of the static dephasing regime theory to superparamagnetic iron-oxide loaded cells," *Magnetic Resonance in Medicine*, vol. 48, pp. 52-61, 2002.

[12] W. Liu and J.A. Frank, "Detection and quantification of magneticlly labeled cells by cellular MRI," *European Journal of Radiology*, vol. In press, 2008.

[13] W.T. Dixon, A.M. Kulkarni, D.E. Meyer, B.C. Bales, and T.K. Foo, "Quantification of SPIO iron: Comparison of three methods," in Proc. 15th Annual Conference of the International Society of Magnetic Resonance In Medicine, 2007, pp. Pages.

[14] R.M. Hoogeveen, C.J.G. Bakker, and M.A. Viergever, "Phase~derivative analysis in MR angiography: Reduced V_{enc} dependency and improved vessel wall detection in laminar and disturbed flow," *Journal of Magnetic Resonance Imaging*, vol. 7, (no. 2), pp. 321-330, 1997.

[15] O. Bomati-Miguel, M.P. Morales, P. Tartaj, J. Ruiz-Cabello, P. Bonville, M. Santos, X. Zhao, and S. Veintemillas-Verdaguer, "Fe-based nanoparticle metallic alloys as contrast agents for magnetic resonance imaging," *Biomaterials*, vol. 26, pp. 5695-5703, 2005.

[16] Wei Liu, Hannes Dahnke, Juergen Rahmer, E. Kay Jordan, and J.A. Frank, "Ultrashort T_2* relaxometry for quantitation of highly concentrated superparamagnetic iron oxide (SPIO) nanoparticle labeled cells," *Magnetic Resonance in Medicine*, vol. 61, (no. 4), pp. 761-766, 2009.